Digital Shadow-based Control of Temperature and Fault Classification in Shell and Tube Heat Exchanger using Fuzzy Logic Technique

Surendran T. Jeyarajah
Department of Electronics and Instrumentation Engineering, SRM Institute of Science and Technology, Kattankulathur, Tamilnadu 603203, India
indravelraajah@gmail.com

G. Joselin Retna Kumar
Department of Electronics and Instrumentation Engineering, SRM Institute of Science and Technology, Kattankulathur, Tamilnadu 603203, India
joselinr@srmist.edu.in (corresponding author)

Received: 13 February 2024 | Revised: 28 February 2024 and 14 March 2024 | Accepted: 18 March 2024

 DOI: https://doi.org/10.48084/etasr.7061

ABSTRACT

In this study, the Digital Shadow (DS) of the Shell and Tube Heat Exchanger (STHE) is designed and analyzed for numerous disturbances that occur when the system is in a running condition. The disruptive segregation of the heat exchanger is related to the DS for its operation, and thus a realistic DS was developed for the STHE. Fuzzy Logic (FL) was used to identify and segregate the disturbance signals from the process output. The Response Optimization (RO) algorithm was adopted and modified to work on the STHE. The observer-based residual generator design was implemented to prevent system failure and defective conditions. Model Predictive Controller (MPC), Transposed System Controller (TSC), and a looping-based control technique called Unity Response Loop (URL) were also implemented, and the results are discussed. The findings of this study contribute to the improvement of the overall performance of non-linear systems in industrial processes and the avoidance of defects.

Keywords-controller design; digital shadow; fuzzy logic; heat transfer

I. INTRODUCTION

The Digital Shadow (DS) of a process encapsulates unique data consisting of observable digital behaviors, activities, impacts, and contacts that have shown evidence on digital devices or cloud-based systems. Generally, the DS monitors the process without visiting the installation field. In addition to that, a process can interact with its DS. This implies that there must be an effective way to share data between the device and its shadow, through either a wired or a wireless channel. Since the communication is better enabled between the process and the DS, the response of the physical system will be replicated in the DS's output. Also, the disturbance that takes place in the system is monitored with the aid of the DS. A Cyber-Physical System (CPS) integrates a physical asset and a digital twin. In industry 4.0, CPS is found to be an important technology to monitor health and production planning [1]. The DS is responsible for collecting data from the machine and generating future data, but in the case of simulation, the generation of new data is impossible. This is the significant difference between the DS and the simulation. The steps to achieve the dynamic process of a heat exchanger are calculated using heat exchange parameters, whereas there are practical constraints involved in the modelling of the heat exchanger. Once the dynamic system is achieved, the next step is to qualify the interaction between the physical system and the designed digital one. This further makes the digital model a DS of the system.

Generally, there are two steps in the classification or diagnosis process. One is fault identification or residual generation, and the other is used to classify the identified faults, mainly depending upon the threshold value. To reduce the deviations occurring in the output response, some kind of control is required. Different types of controllers are employed to control these deviations. Every industrial process has different types of faults or disturbances in its output. Similarly, hydraulic systems have some common faulty conditions. Faults are defined as the difference between the actual and the desired result/ouput. Leakages in pipelines, calibration errors in sensors, and environmental conditions are the most common causes which change the system parameters and cause malfunctions in the hydraulic systems [2]. Based on the fault tolerance property, fault failures are majorly ranked into two categories, namely partial fault failures and total fault failures. When a process has an abnormality, a specific diagnostic classifier will be employed to picturize the faults. Finding,

separation, and categorization are the three important key points of fault analysis which will be primarily done through the modeling of a physical system. In this work, the proposed idea is to perform fault analysis through the DS.

By setting a variable or fixed threshold value on the generated residual signals, the faults are detected with the help of the DS and the difference between the actual measurements and the estimated output is noted. The system can be addressed as a residual generator if an algorithm is employed to generate the residuals [3]. Generation and analysis of the residuals can be completed through fuzzy logic. However, in this paper, the Luenberger Observer is deployed to generate the residuals [4] and the fuzzy logic system analyzes them. A non-zero D matrix represents a system with a transfer function with a relative degree of zero and the same number of poles as zeros. The magnitude of the output would reach a constant value at very high frequencies instead of zero. In general, the looping concept is introduced to reduce the error value of the process. Nevertheless, the proposed URL [5] significantly decreases the error and makes the output resemble the desired input using the former's algorithm without the application of any external controllers. Also, this method does not affect the dynamics of the digital system, which receives the data from the physical system.

II. DATA ACQUISITION AND PARAMETER ESTIMATION

An industrial IoT-based sensor system is deployed to acquire the physical parameters of the heat exchanger. A DS should relate to the physical system to collect the information through the proper communication channel [6, 7]. The digital system will work based on the collected parameters from the real system. A suitable parameter estimation algorithm should be adopted to calculate the values. The Logarithmic Mean Temperature Difference (LMTD) is selected to calculate the overall heat transfer coefficient.

III. OPTIMAL PID CONTROL

Optimization is the process of selecting the most appropriate range or value for adjustable parameters. Within the optimization plane, the appropriate parameter value is chosen and utilized to achieve the desired output. There is an increasing variety of optimization methods available for purchase. The Response Optimization (RO) technique is a straightforward and efficient approach for optimizing the parameters. The PID controller manages the virtual heat exchanger by the utilization of the RO algorithm. Nevertheless, it is intricate and characterized by strong non-linearity. The PID controller, optimized and tuned using the RO algorithm, is utilized to regulate the digital representation of the heat exchanger. The controller's settings are detailed in Table I.

TABLE I. CONTROLLER PARAMETERS

	PID	Optimal PID
Kp	0.3674	0.0980
Ki	2.1552	1.0923
Kd	1.0215	0.2533

IV. MODEL PREDICTIVE CONTROL

The controlled variable should be specific and have a desired value. The process model is implemented to achieve that, and it calculates the perfect changes of the Manipulated Variables (MVs) [8]. Now the model is replaced by the DS of the system. The output variables are measured at all time instants. After that, the optimization algorithm is applied to compute the associated alterations in the MVs for some instants in the future [9, 10].

The changes are made first, and the controlled variables have a certain effect due to these changes. At the next time instant, the optimization problem receives the new values of the measured controlled signals to get the updated values of the MVs.

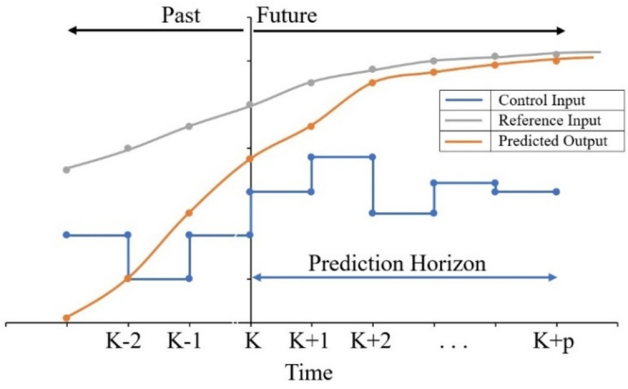

Fig. 1. Model predictive control horizons.

V. TRANSPOSED SYSTEM CONTROL

The proposed Transposed System (TS) controller is very powerful when compared to the other classical controllers. It is designed in such a manner that it will effectively reduce the error value. The TS controller achieves the best results with a simple arrangement and by simply transposing the A, B, C, and D matrices. The structure of the TS controller is depicted in Figure 2. The controller structure is equivalent to that of the state-space model of the process. The TS controller is mathematically represented in (1) and (2):

$$x'_{TS}(t) = A^T x(t) + C^T e(t) \quad (1)$$

$$u(t) = B^T x(t) + D^T e(t) \quad (2)$$

From the structure portrayed in Figure 2 $e(t) = r(t) - y(t)$=>

$$u(t) = B^T x(t) + D^T[r(t) - y(t)]$$

$$u(t) = B^T x(t) + D^T[r(t) - (Cx(t) + Du(t))]$$

$$u(t) = B^T x(t) + D^T r(t) - D^T C x(t) - D^T D u(t)$$

$$u(t) = [B^T - D^T C]x(t) + D^T r(t) - D^T D u(t)$$

$$u(t) + D^T D u(t) = [B^T - D^T C]x(t) + D^T r(t)$$

$$[I + D^T D]u(t) = [B^T - D^T C]x(t) + D^T r(t)$$

$$u(t) = \left[\frac{[B^T - D^T C]}{[I + D^T D]}\right] x(t) + \left[\frac{D^T}{[I + D^T D]}\right] r(t)$$

$$u(t) = \left[\frac{[B^T - D^T C]}{I} + \frac{[B^T - D^T C]}{D^T D}\right] x(t) + \left[\frac{D^T}{I} + \frac{D^T}{D^T D}\right] r(t)$$

$$u(t) = \left[\frac{[B^T - D^T C]}{I} + \frac{B^T}{D^T D} - \frac{D^T C}{D^T D}\right] x(t) + \left[\frac{D^T}{I} + \frac{D^T}{D^T D}\right] r(t)$$

$$u(t) = [B^T - D^T C + B^T (D^T D)^{-1} - C D^{-1}]\, x(t) + [D^T + D^{-1}] r(t) \quad (3)$$

where u(t) is the controller output that goes to the system as an input. To get the system response for the input u(t), (3) is substituted by output y(t) and state x(t).

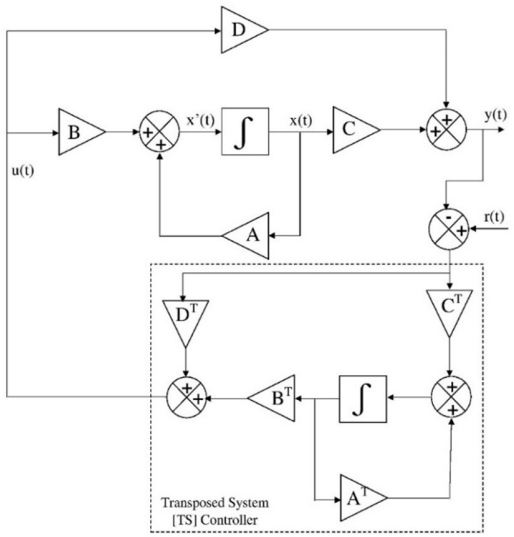

Fig. 2. Structure of the TS controller.

$$y(t) = Cx(t) + Du(t)$$

$$y(t) = Cx(t) + D[[B^T - D^T C + B^T (D^T D)^{-1} - C D^{-1}]\, x(t) + [D^T + D^{-1}] r(t)]$$

$$y(t) = Cx(t) + [D B^T - D D^T C + D B^T (D^T D)^{-1} - D C D^{-1}]\, x(t) + [D D^T + D D^{-1}] r(t)$$

$$y(t) = [C + D B^T - D D^T C + D B^T (D^T D)^{-1} - D C D^{-1}]\, x(t) + [D D^T + D D^{-1}] r(t) \quad (4)$$

$$x'(t) = Ax(t) + Bu(t)$$

$$x'(t) = Ax(t) + B[[B^T - D^T C + B^T (D^T D)^{-1} - C D^{-1}]\, x(t) + [D^T + D^{-1}] r(t)]$$

$$x'(t) = Ax(t) + [B B^T - B D^T C + B B^T (D^T D)^{-1} - B C D^{-1}]\, x(t) + [B D^T + B D^{-1}] r(t)$$

$$x'(t) = [A + B B^T - B D^T C + B B^T (D^T D)^{-1} - B C D^{-1}]\, x(t) + [B D^T + B D^{-1}] r(t) \quad (5)$$

For a better understanding, (4) and (5) are rewritten as (6) and (7):

$$x'(t) = A^* x(t) + B^* r(t) \quad (6)$$

$$Y(t) = C^* x(t) + D^* r(t) \quad (7)$$

where:

$$A^* = A + B B^T - B D^T C + B B^T (D^T D)^{-1} - B C D^{-1}$$

$$B^* = B D^T + B D^{-1}$$

$$C^* = C + D B^T - D D^T C + D B^T (D^T D)^{-1} - D C D^{-1}$$

$$D^* = D D^T + D D^{-1}$$

These are the state, input, output, and direct feedthrough matrices with the impact of the TS controller, respectively. The closed-loop gains (A^*, B^*, C^*, and D^*) are investigated through calculating the observability and controllability matrices and ranks. This results in a system with the TS controller being fully observable and fully controllable.

VI. UNITY CONTROL LOOP

Unity Response Loop (URL) is a simple looping concept that can control any system in a very strong manner. URL applies to both transfer function and state-space models. To control the system, the URL is not going to use any components from the system. The structure of the URL is exhibited in Figure 3.

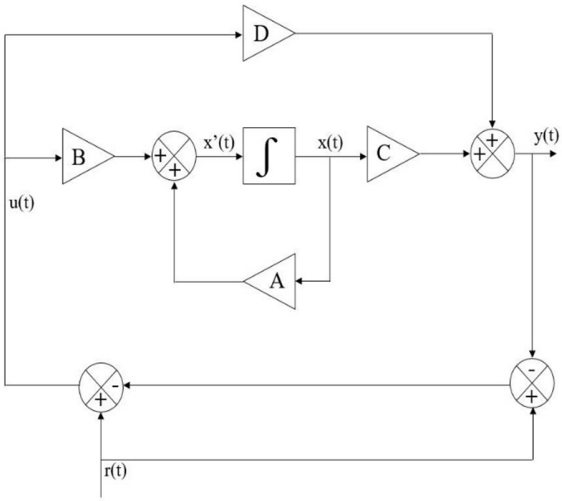

Fig. 3. Structure of the URL controller.

$$u(t) = r(t) - [r(t) - y(t)]$$

$$u(t) = r(t) - r(t) + y(t)$$

$$u(t) = y(t) \quad (8)$$

Equation (8) is substituted by the output equation y(t):

$$y(t) = Cx(t) + Dy(t)$$

$$y(t) - Dy(t) = Cx(t)$$

$$[I - D] y(t) = Cx(t)$$

$$y(t) = \left[\frac{C}{I - D}\right] x(t)$$

$$y(t) = \left[\frac{C}{1} - \frac{C}{D}\right] x(t)$$

$$y(t) = [C - C D^{-1}] x(t) \quad (9)$$

Equation (8) is substituted by the in state equation x'(t):

$$x'(t) = Ax(t) + By(t) \quad (10)$$

Equation (9) is substituted in (10):

$$x'(t) = Ax(t) + B[[\mathrm{C} - \mathrm{CD}^{-1}]\mathrm{x(t)}]$$

$$x'(t) = Ax(t) + [B\mathrm{C} - B\mathrm{CD}^{-1}]\mathrm{x(t)}$$

$$x'(t) = [A + B\mathrm{C} - B\mathrm{CD}^{-1}]\mathrm{x(t)} \quad (11)$$

where:

$$A + B\mathrm{C} - B\mathrm{CD}^{-1} = A^{\odot}$$

$$\mathrm{C} - \mathrm{CD}^{-1} = B^{\odot}$$

So, (9) and (11) can be written as:

$$\mathrm{x'(t)} = \mathrm{A}^{\odot}\mathrm{x(t)} \quad (12)$$

$$\mathrm{y(t)} = \mathrm{B}^{\odot}\mathrm{x(t)} \quad (13)$$

Equations (12) and (13) are, respectively, the state and output equations of the closed loop system with URL. These equations explain the effect of URL on a state space model. Both equations are only affected by the state x(t).

VII. FAULT CLASSIFICATION

An undetermined fluctuation from the standard, acceptable, or usual condition of at least one system parameter or process characteristic property is called a fault. To ensure mapping is performed to confirm the robustness of inherent fluctuation in the detected trends, the fuzzy reasoning technique is proposed [11-12]. Fault diagnosis includes identification of the type, location, time, and size of the detected fault. A collection of physically interchangeable if-then rules, collectively known as the fuzzy rule base (Figure 4), interfere with the process. They are used to estimate the amplitude of faults [13]. The residuals generated and the threshold values (Table II) for three different faults are given as inputs to the fuzzy system.

TABLE II. MAGNITUDE RANGE AND ITS RESPECTIVE FAULT TYPE

Magnitude Range (dB)	Sensor fault	Actuator fault	Process fault
0 to 10	-	-	✓
10 to 15	-	✓	-
15 to 40	✓	-	-
< 0	-	-	-

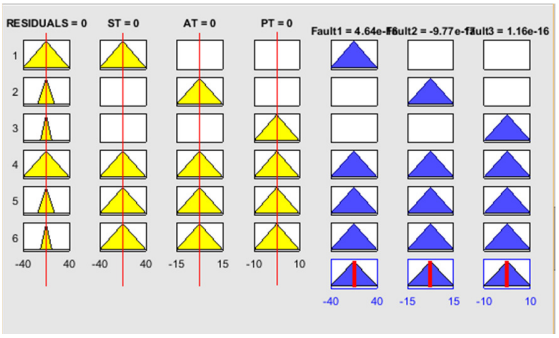

Fig. 4. Fuzzy rule viewer for the classification of different faults from the generated residual signal.

Based on the threshold values, the residual is classified into 3 different types (Table III). The classified faults are sensor fault, actuator fault, and process fault [14].

TABLE III. FAULT TYPE AND ITS VALUE

Type of fault	Value given by fuzzy logic
Sensor Fault	4.64e−16
Actuator Fault	−9.77e−17
Process Fault	1.16e−16

VIII. RESULTS

The DS of the shell and tube heat exchanger is successfully designed and compared with the output of the physical heat exchanger. The shadow gets data from the physical system and works based on the controller actions. To obtain the response of the DS, controllers, such as optimal PID, Model Predictive Control (MPC), Transposed System Controller, and Unity Response Loop are proposed. The effect of the Optimal PID controller on cold liquid temperature is manifested in Figure 5.

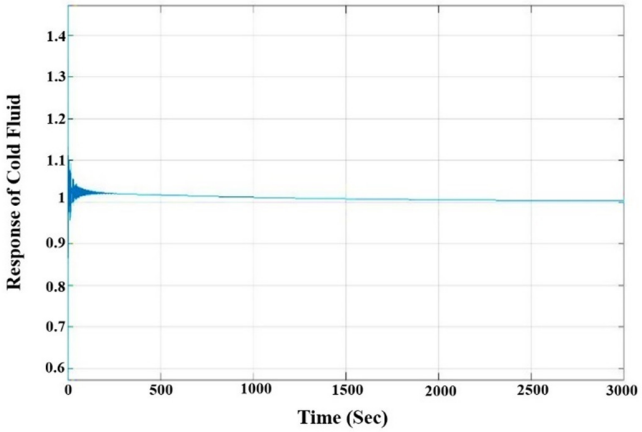

Fig. 5. The cold fluid output temperature.

The Optimal PID controller is powered by the response optimization algorithm, which gives the controlled output or the approximately desired output [15]. Figure 6 illustrates the hot output of the heat exchanger with the optimal PID control action.

The responses are settled, but the settling time is very high. Because of this, the DS took much time to make decisions on the physical system. The MPC algorithm was implemented to reduce the setting time. The open-loop response of the TITO transfer function model of the heat exchanger is detected in Figure 7.

Since the response is obtained through the linearized model, the system gives the settled output, but the responses widely deviate from the respective desired setpoints.

The MPC fabulously contributed to reducing the settling time of the response. In Figure 8, the response of the cold fluid output temperature is followed in every instance and settles near to it with a small-time difference [16].

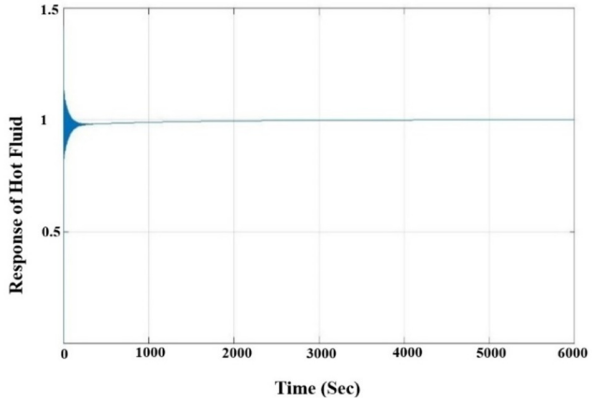

Fig. 6. Hot fluid output temperature.

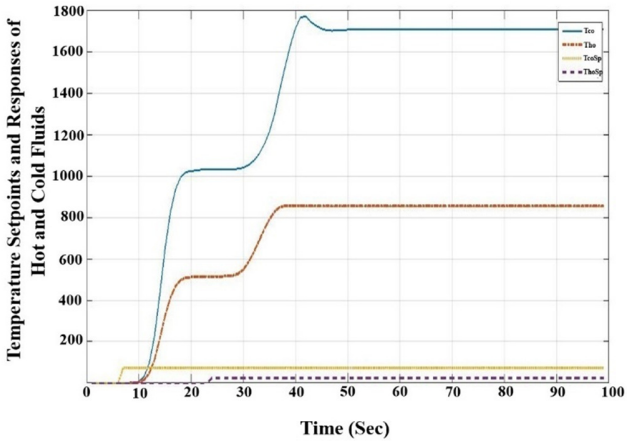

Fig. 7. Open loop response of the system along with its setpoints.

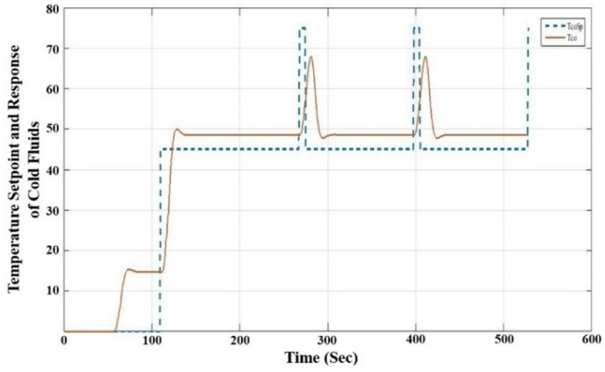

Fig. 8. The effect of MPC on the response of cold fluid output temperature with its setpoint.

Figure 9 demonstrates the effect of the MPC controller on the responses of the cold and hot fluid outlet temperatures. Depending upon the step-change in the reference signal, the servo tracking of cold inlet flow rate takes place on the response of the system as the MPC control action. The controller makes the manipulated variables attain the reference value in all step changes [17]. Once the error value is minimized, the controller renders the MVs stable. To get an error-free response and overcome the drawbacks of Optimal PID and MPC, the TS controller is proposed.

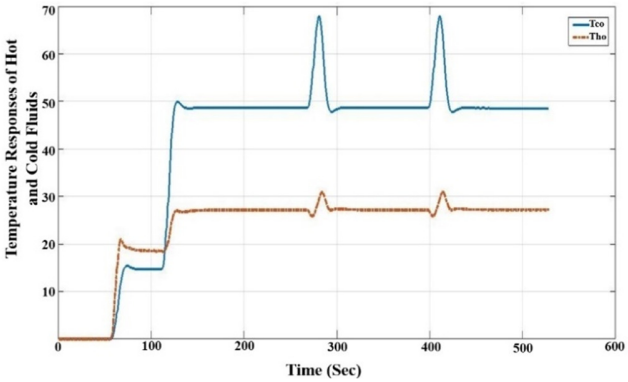

Fig. 9. Controlled responses of cold and hot fluid outlet temperatures.

The final response of the TS controller is spotted in Figure 10. The input change is occurring at t = 4. After that, the controller is making the system response follow the reference signal r(t). This quality makes the TS controller more suitable for controlling linear time-invariant systems. The system response is exactly settled on the reference signal provided to the system. Figure 10 shows that the controller extremely minimized the error e(t). Every controller's performance is determined based on the error value and the acquired value of the error is very close to zero.

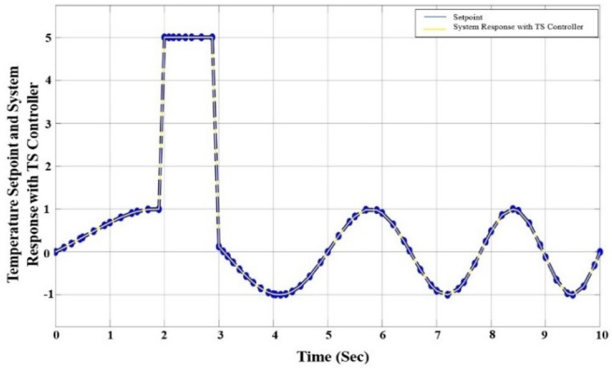

Fig. 10. Setpoint vs response of the system with the TS controller.

If the error value is minimal, then the controller performance is considered good. The proposed TS controller works well on the system with and without the D matrix.

The URL does not depend on the effect of the input u(t). So, the equations do not consist of the input matrix B and the direct feedthrough matrix D. URL eliminates the D matrix from the output equation. The system output y(t) is equal to the value of the input, u(t). At t = 0, the u(t) is equal to r(t). It is obvious that y(t) = r(t) Since u(t) = r(t) at the initial state, the output equation is fully dependent on the value of x(t). So, it produces the actual reference signal r(t) as the output y(t).

The obtained response from the system with the URL is displayed in Figure 11. The output y(t) replicates the reference signal r(t). A fuzzy inference system is used to classify the residuals generated by the Luenberger Observer. The Luenberger Observer takes the DS's input and the output signals as input.

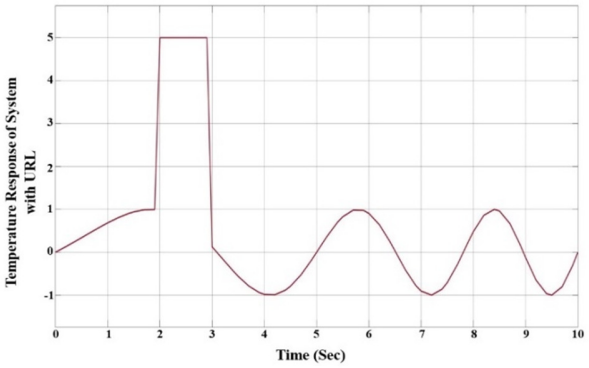

Fig. 11. System response with the URL controller.

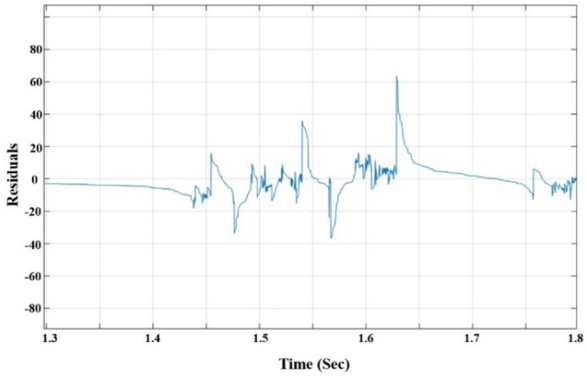

Fig. 12. Residual signal generated by the Luenberger Observer.

Based on this signal, the Luenberger Observer generates the residual signal as disclosed in Figure 12. However, the identified residual signal consists of more than one faults. The combined signal is given to FIS to segregate the faults from the residual signal. The fuzzy rule base will be used to classify the faults from the residual signal. The rules are constructed in terms of membership functions. They could be classified based on the amplitude of faults.

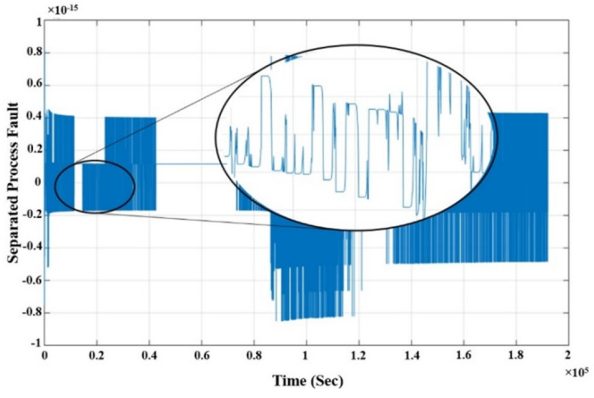

Fig. 13. Segregated process fault.

A total of three faults are segregated from the residual signal utilizing FIS. Out of them, the process fault is exhibited in Figure 13. Given that the amplitude is very low, the fuzzy system gives a complex waveform. The other two faults have a negligible effect on the process. Considering this, only the process fault is presented in this paper.

IX. CONCLUSION

This study focused on the design and examination of the Digital Shadow (DS) of a heat exchanger in conjunction with a physical shell and tube heat exchanger. The integration of an IoT-based sensor unit facilitated data collection, bringing the DS to life. Through the application of a response optimization algorithm, the parameters of the PID controller were fine-tuned to mitigate process interaction inherent in MIMO systems. The optimized PID controller, powered by the response optimization algorithm, ensured system responses were stable and accurately settled at the reference value. To further enhance performance, Model Predictive Control (MPC) was introduced to minimize the settling time, resulting in quicker attainment of steady-state values. The proposed Transposed System (TS) controller exhibited superior response compared to both Optimal PID and MPC, delivering precise and prompt responses without delays at the setpoint. Additionally, the effectiveness of the fuzzy-based fault segregation was demonstrated, successfully identifying and classifying major faults based on their amplitude.

This study competently uses the DS to regulate the heat exchanger mechanism. The integrated approach optimized controller parameters and shortened the settling time, enhancing control and fault detection capabilities. With the goal of improving the heat exchanger system performance and reliability, this research offers significant new insights into the implementation of advanced control techniques and DS.

REFERENCES

[1] S. M. E. Sepasgozar, "Differentiating Digital Twin from Digital Shadow: Elucidating a Paradigm Shift to Expedite a Smart, Sustainable Built Environment," *Buildings*, vol. 11, no. 4, Apr. 2021, Art. no. 151, https://doi.org/10.3390/buildings11040151.

[2] N. A. Khan, M. Sulaiman, P. Kumam, and M. A. Bakar, "Thermal Analysis of Conductive-Convective-Radiative Heat Exchangers With Temperature Dependent Thermal Conductivity," *IEEE Access*, vol. 9, pp. 138876–138902, 2021, https://doi.org/10.1109/ACCESS.2021.3117839.

[3] A. Noshadi, J. Shi, W. S. Lee, P. Shi, and A. Kalam, "Optimal PID-type fuzzy logic controller for a multi-input multi-output active magnetic bearing system," *Neural Computing and Applications*, vol. 27, no. 7, pp. 2031–2046, Oct. 2016, https://doi.org/10.1007/s00521-015-1996-7.

[4] A. Guerra de Araujo Cruz, R. Delgado Gomes, F. Antonio Belo, and A. Cavalcante Lima Filho, "A Hybrid System Based on Fuzzy Logic to Failure Diagnosis in Induction Motors," *IEEE Latin America Transactions*, vol. 15, no. 8, pp. 1480–1489, 2017, https://doi.org/10.1109/TLA.2017.7994796.

[5] T. Surendran, K. Nandini, R. Nagalakshmi, and J. Johnsi, "Design Materials for Unity Control Loop," *IOP Conference Series: Materials Science and Engineering*, vol. 993, no. 1, Sep. 2020, Art. no. 012089, https://doi.org/10.1088/1757-899X/993/1/012089.

[6] A. Rasheed, O. San, and T. Kvamsdal, "Digital Twin: Values, Challenges and Enablers From a Modeling Perspective," *IEEE Access*, vol. 8, pp. 21980–22012, 2020, https://doi.org/10.1109/ACCESS.2020.2970143.

[7] A. Ladj, Z. Wang, O. Meski, F. Belkadi, M. Ritou, and C. Da Cunha, "A knowledge-based Digital Shadow for machining industry in a Digital Twin perspective," *Journal of Manufacturing Systems*, vol. 58, pp. 168–179, Jan. 2021, https://doi.org/10.1016/j.jmsy.2020.07.018.

[8] M. S. S. Asadi, H. Afarideh, M. Ghergherechi, and J. S. Chai, "Model Predictive Control-Based Smart Linear Servo-Motor Driver for a Resonance Frequency Tuner of Azimuth Variable Field Cyclotrons," *Journal of the Korean Physical Society*, vol. 76, no. 7, pp. 592–594, Apr. 2020, https://doi.org/10.3938/jkps.76.592.

[9] L. Dong, L. Dou, J. Chen, and Y. Xia, "Hybrid model predictive control for speed control of permanent magnet synchronous motor with saturation," *Journal of Control Theory and Applications*, vol. 9, no. 2, pp. 251–255, May 2011, https://doi.org/10.1007/s11768-011-8016-y.

[10] K. H. Cho, Y. K. Yeo, J. S. Kim, and S. Koh, "Fuzzy model predictive control of nonlinear pH process," *Korean Journal of Chemical Engineering*, vol. 16, no. 2, pp. 208–214, Mar. 1999, https://doi.org/10.1007/BF02706838.

[11] H. Wang, Y. Kang, L. Yao, H. Wang, and Z. Gao, "Fault Diagnosis and Fault Tolerant Control for T–S Fuzzy Stochastic Distribution Systems Subject to Sensor and Actuator Faults," *IEEE Transactions on Fuzzy Systems*, vol. 29, no. 11, pp. 3561–3569, Aug. 2021, https://doi.org/10.1109/TFUZZ.2020.3024659.

[12] E. A. Esleman, G. Önal, and M. Kalyoncu, "Optimal PID and fuzzy logic based position controller design of an overhead crane using the Bees Algorithm," *SN Applied Sciences*, vol. 3, no. 10, Sep. 2021, Art. no. 811, https://doi.org/10.1007/s42452-021-04793-0.

[13] X. Weng, J. Zhang, and Y. Ma, "Path Following Control of Automated Guided Vehicle Based on Model Predictive Control with State Classification Model and Smooth Transition Strategy," *International Journal of Automotive Technology*, vol. 22, no. 3, pp. 677–686, Jun. 2021, https://doi.org/10.1007/s12239-021-0063-x.

[14] B. Pyun, M. Seo, S. Kim, and H. Choi, "Development of an Autonomous Driving Controller for Articulated Bus Using Model Predictive Control Algorithm with Inner Model," *International Journal of Automotive Technology*, vol. 23, no. 2, pp. 357–366, Apr. 2022, https://doi.org/10.1007/s12239-022-0033-y.

[15] A. A. Kapse, V. C. Shewale, S. D. Barahate, A. B. Kakade, and S. J. Surywanshi, "Experimental Investigation of Heat Transfer and Pressure Drop Performance of a Circular Tube with Coiled Wire Inserts," *Engineering, Technology & Applied Science Research*, vol. 14, no. 1, pp. 12512–12517, Feb. 2024, https://doi.org/10.48084/etasr.6551.

[16] H. V. Nguyen, F. Deng, and T. D. Nguyen, "Optimal FLC-Sugeno Controller based on PSO for an Active Damping System," *Engineering, Technology & Applied Science Research*, vol. 14, no. 1, pp. 12769–12774, Feb. 2024, https://doi.org/10.48084/etasr.6662.

[17] S. Barhate, R. Mudhalwadkar, and S. Madhe, "Fault Detection Methods Suitable for Automotive Applications in Proton Exchange Fuel Cells," *Engineering, Technology & Applied Science Research*, vol. 12, no. 6, pp. 9607–9613, Dec. 2022, https://doi.org/10.48084/etasr.5262.